K_v = volume shape factor
L = particle size, linear
M = mass of solids in suspension, mass/unit volume
N^o = number of nuclei
n = population density, numbers/unit length
n^o = population density of nuclei
Q = feed or product rate, volume/unit time
r = linear growth rate
s = supersaturation
T = residence time
t = time
V = crystallizer volume
ρ = crystal density

LITERATURE CITED

1. Bransom, S. H., W. J. Dunning, and B. Millard, *Discussions Faraday Soc.*, **5**, 83 (1949).
2. Murray, D. C., Ph.D. thesis, Iowa State Univer., Ames, Iowa (1964).
3. Powers, Harold E. C., *Ind. Chemist* 351 (July 1963).
4. Randolph, A. D., *AIChE J.*, **11**, 424 (1965).
5. Randolph, A. D., and M. A. Larson, *ibid.*, **8**, 639 (1962).
6. Schoen, H. M., *Ind. Eng. Chem.*, **53**, 607 (1961).
7. Timm, D. C., MS thesis, Iowa State Univer. (1965).
8. Timm, D. C., and M. A. Larson, *AIChE J.*, **14**, 452 (1968).

Manuscript received February 2, 1967; revision received September 6, 1967; paper accepted September 12, 1967. Paper presented at AIChE Houston meeting.

Effect of Nucleation Kinetics on the Dynamic Behavior of a Continuous Crystallizer

DELMAR C. TIMM and MAURICE A. LARSON
Iowa State University of Science and Technology, Ames, Iowa

The nucleation kinetics of three materials were related to the growth kinetics using steady state data obtained at various degrees of supersaturation. The power models obtained from the three crystallizations exhibited widely different kinetic orders. These materials were then crystallized under unsteady state conditions in a mixed suspension–mixed product removal crystallizer and the transient size distributions were determined. The unsteady state model previously developed by Randolph and Larson was solved on a digital computer for the three systems. Good agreement was obtained. It was found that unsteady state experiments have some advantages over steady state experiments in determining the kinetic order of nucleation.

Experimental growth and nucleation rate data that are relevant to the behavior of crystal size distribution in industrial continuous crystallizers, and descriptions of methods for obtaining such data are woefully lacking in the literature. Classical methods for measuring growth rates usually utilize an experiment only where growth occurs on a single crystal or on a suspension of monosized crystals. Conditions selected are such that little or no nucleation occurs. Nucleation experiments are conducted in a way that is even further removed from reality. They are usually carried on by inducing nucleation in a previously clear nuclei free solution under conditions of supersaturation that vary during the experiment. In a continuous industrial crystallizer, nucleation and growth are taking place hopefully under constant conditions of temperature, pressure, and supersaturation.

An extensive analysis of mixed suspension, mixed product removal, and continuous crystallization has been performed by Randolph and Larson (*8*). A model was developed from a basic numbers balance, to predict and analyze transient as well as steady state behavior for such a crystallization system. The following equation predicts the transient response for unsteady state operating conditions:

$$\frac{\partial n}{\partial t} = -r\frac{\partial n}{\partial L} - \frac{n}{T} \qquad (1)$$

The characterizing parameter is population density, n, which is defined by

$$\Delta N = \int_{L_1}^{L_2} n \, dL \qquad (2)$$

At steady state, Equation (1) simplifies to

$$n_o = n_o^o \exp\left(-L/r_o T_o\right) \qquad (3)$$

Equation (3) has been used by several authors (*1, 6, 9*) in the analysis of factors that affect size distribution in continuous crystallizers.

In the development of the model, it was assumed that the following constraints were imposed on the system: no crystal seeding, perfectly mixed crystal suspension, mixed product removal, and isothermal environment. It was further assumed that McCabe's ΔL Law applied and the fluid properties were constant.

The assumption that McCabe's ΔL Law does hold is quite necessary for ease in solution of the model, but it does impose some limitations on the applicability of the results. McCabe (*3*) observed that under a variety of operating conditions, crystal growth rate is independent of particle size. However, later observations have shown that large deviations from this law may occur if diffusional resistance is a dominant factor in the crystal growth mechanism. McCabe and Stevens (*4*) reported that the law did not apply for the crystallization of copper sulfate. In their investigation a monosized sample of crystals was placed on a retaining screen and grown for a period of time. The growth rates for various sized crystals, all subjected to a similar environment, were calculated from a material balance.

In these experiments crystals subjected to different fluid velocities grew at different rates, but different sized crystals grew at a constant rate when subjected to a constant fluid velocity. In a suspended magma sample, large crystals may be subjected to a higher relative settling velocity than small ones. Consequently, growth rate may be expected to be a function of particle size. However, similar conditions may not be approximated in commercial crystallizers. The latter may be more accurately characterized by high magma concentrations so that free settling laws do not apply, but rather a condition of hindered settling does exist. In this case, growth rate as a function of crystal size will be much less probable. Data collected in this investigation indicate that for the three crystal systems analyzed, McCabe's ΔL Law is a valid assumption.

For a crystallizer operated at constant volume, a mass balance gives the following relationship between crystal growth rate, residence time, solution concentration changes, and suspension area:

$$r = \frac{K(\Delta C)}{T \int_0^\infty nL^2 dL} \tag{4}$$

This equation along with the kinetic equations which relate growth and nucleation rates with supersaturation (*6*) shows that there is a dynamic interrelationship between size distribution and the factors that determine this distribution, namely growth rate and nucleation rate.

Murray and Larson (*5*) developed a continuous, mixed suspension, mixed product removal, salting out crystallizer, satisfying the constraints and assumptions incorporated in the development of Equations (1) and (3), for the purpose of collecting steady state and transient data in order to analyze this model. An ammonium alum-ethanol-water system was investigated as this system developed regular octahedral crystals with relatively high growth rates. In this investigation the work of Murray and Larson was elaborated to include three crystal systems which exhibit widely varying kinetic orders for their respective nucleation rates. These systems involved an extension of the investigation of the alum system, plus an investigation of ammonium sulfate-methanol-water and sodium chloride-ethanol-water systems. These three solutes are of commercial importance in present day crystallization processes. The systems provided crystals of regular habits that could be conveniently analyzed by conventional sieve analysis; this was in conjunction with a Coulter Counter procedure specifically designed to analyze crystals down to 10 to 20 μ in size. The specific gravity and maximum particle size obtained permitted close approximation of a perfectly mixed, continuous suspension. The salting out agents were selected so that a single liquid phase was present for all operating conditions.

DATA REDUCTION

The salting out crystallization system used for this investigation has previously been described by Murray and Larson (*5*). The larger sized crystals were analyzed by a conventional sieve analysis. The smaller sized crystals, less than 0.2 mm. in diameter, were analyzed on a Coulter Counter. Repeated analysis of steady state distributions for a given experiment resulted in highly reproducible data. In addition repeated steady state experiments lead to reproducible data.

STEADY STATE RESULTS

Equation (3) indicates that if a crystallizer is operating at steady state, a plot of the log of the population density vs. crystal size should result in a straight line with a slope proportional to $-1/r_oT_o$ and an intercept equal to the log of the nuclei population density. A set of experiments performed at different residence times provides data which

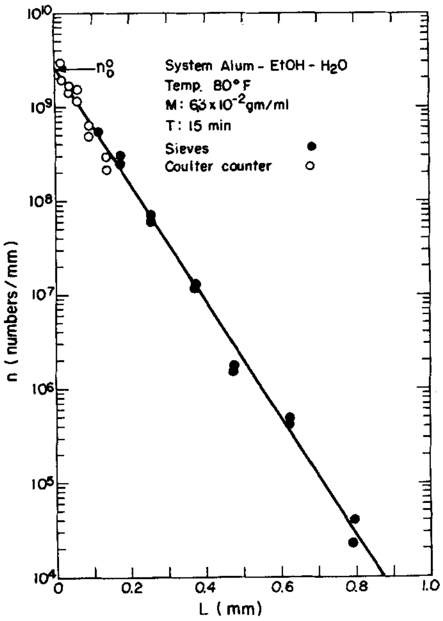

Fig. 1. Steady state crystal size distribution, alum-ethanol-water.

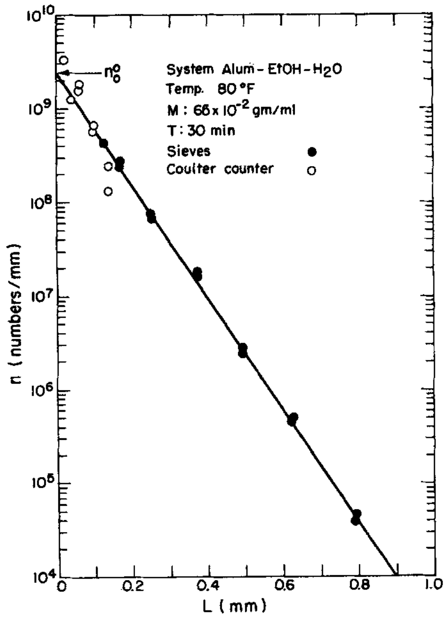

Fig. 2. Steady state crystal size distribution, alum-ethanol-water.

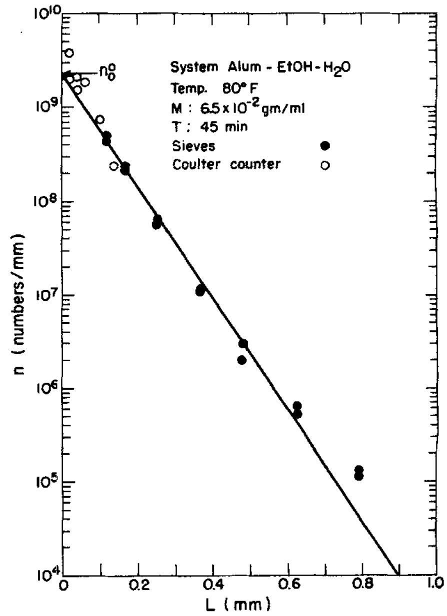

Fig. 3. Steady state crystal size distribution, alum-ethanol-water.

can be used to correlate growth rate as a function of nuclei population denstiy, n_o^o. This follows because of the constraint on the system. A change in residence time will cause a change in supersaturation and consequently a change in growth and nucleation rate.

Murray and Larson (5) showed that data collected at different residence times holding all other operating parameters constant, including suspension density, can be correlated by the following relationships:

$$\frac{dN^o}{dt} = n^o r = K r^i \tag{5}$$

$$n^o = K r^{i-1} \tag{6}$$

Thus, a plot of the log of the nuclei population density vs. the log of the growth rate at different residence times, will give a straight line with a slope related to the kinetic order of the nucleation rate, namely i of Equation (5). The proportionality of constant K, is a function of operating conditions that include temperature, degree of agitation suspension density, and fluid characteristics which effect this basic mass transfer process. In another investigation Larson, et al. (2) have expanded on this study to include the effects of suspension density on nucleation rates.

Figures 1, 2 and 3 are steady state graphs for the alum system at 15, 30 and 45 min. residence times. Figures 4 and 5 present similar data for the ammonium sulfate and sodium chloride systems. These graphs demonstrate the continuity of data obtained by the two analyzing techniques. Pertinent experimental information is summarized in Table 1 for the three systems. Figure 6 shows the linear correlation of the log of the nuclei population density vs. the log of the growth rate for the three systems, as predicted by Equation (6). The results of this analysis indicate that the kinetic order of the nucleation rate for the three crystal systems are 1.0 for alum, 4.0 for ammonium sulfate, and 9.0 for sodium chloride. Robinson and Roberts (8) also reported a kinetic order of 4.0 for the reaction crystallization of ammonium sulfate.

Recalling that the kinetic order of Equation (5) is numerically equal to the slope of the graph of the log of the nuclei population density vs. the log of the growth rate plus one, a brief discussion of the evaluation method used to obtain these results is pertinent. Figures 1 through 5 are semilogarithmic graphs, log population density as ordinate and average crystal size as abscissa. Growth rates for the respective systems at different residence times are proportional to the slopes of these graphs; the intercepts are equal to the log of the nuclei population density. Noting the scattering of data, the best straight line is not always obvious. Small variations in the construction of these lines have but a slight effect on the numerical value of the growth rates, but significantly affect the numerical value for the nuclei population density. Therefore, the following procedure was developed to determine the best straight line.

Suspension density is expressed in terms of population density by the following relationship:

$$M = \frac{K_v \rho \int_o^\infty n L^3 dL}{V} \tag{7}$$

At steady state, Equation (3) is applicable. Thus, Equation (7) may be reduced to the following:

$$M = \frac{6 \rho K_v (r_o T_o)^4 n_o^o}{V} \tag{8}$$

A trial and error procedure was then used to adjust the lines so that the calculated suspension density from Equation (8) agreed with that observed experimentally.

The population densities for the larger size fractions often lie above these straight lines as shown by the steady state graphs. Microscopic examination indicated that a significant part of these large crystals were really agglomerations. Therefore, their numerical value would be expected to lie above the linear relationship. However, the weight of these large size fractions were but a few percent of the total weight of a given sample.

The dominant particle size of a distribution obtained under the conditions of these experiments is given by

$$L_d = 3 r T \tag{9}$$

Dominant particle sizes, which may be used as measures of crystal size distribution enhancement caused by increasing residence times, are tabulated in Table 1. Figures 1 through 5 also demonstrate this size distribution enhancement as a function of residence time and also as a function of the kinetic order of the nucleation rate. The

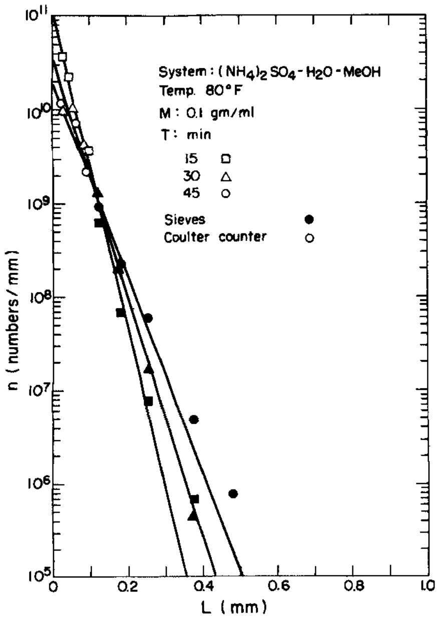

Fig. 4. Steady state crystal size distribution, ammonium sulfate-methanol-water.

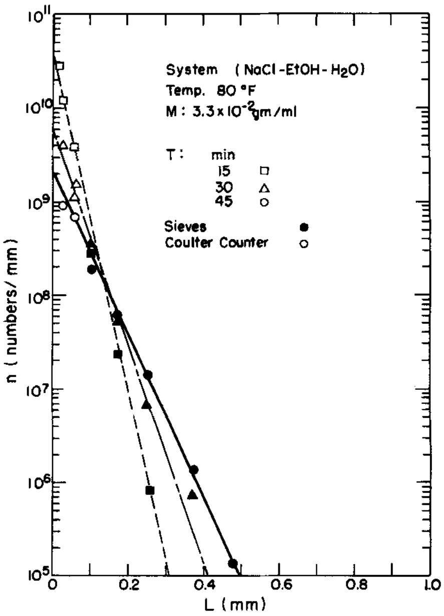

Fig. 5. Steady state crystal size distribution sodium chloride-ethanol-water.

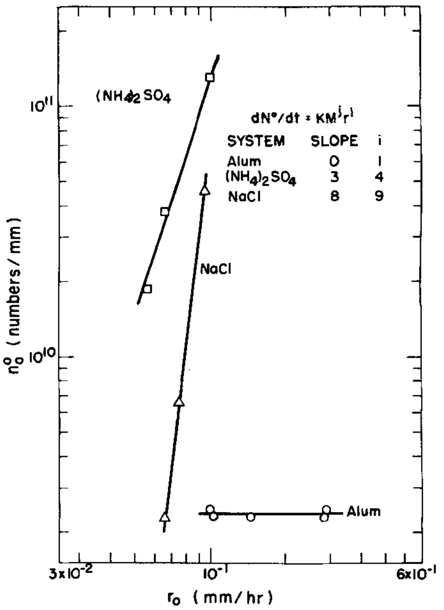

Fig. 6. Nucleation kinetics.

TABLE 1. EXPERIMENTAL OPERATING CONDITIONS AND OBSERVATIONS

System	T hr.	M g. solid 100 ml. slurry	Temp. °F.	Feed Conc., g. solute 100 ml. water	Feed alcohol ratio	r mm./hr.	$n_o^o \times 10^{-10}$ No./mm.	L_d mm.
Alum								
steady state	0.25	6.3	80	10	3/1	0.284	0.23	0.213
	0.50	6.5	80	10	3/1	0.146	0.23	0.219
	0.75	6.5	80	10	3/1	0.099	0.24	0.222
transient	0.25	5.9	80	10	5/1	0.291	0.22	0.218
	0.75	6.0	80	10	5/1	0.102	0.23	0.230
Ammonium sulfate	0.25	11.0	80	57	10/3	0.100	13.00	0.075
	0.50	10.0	80	57	10/3	0.068	3.80	0.102
	0.75	12.0	80	57	10/3	0.056	1.90	0.126
Sodium chloride	0.25	3.3	80	34	5/1	0.094	4.50	0.071
	0.50	3.3	80	34	5/1	0.075	0.65	0.113
	0.75	3.3	80	34	5/1	0.066	0.23	0.148

higher the kinetic order, the greater is the effect of residence time on the size distribution enhancement.

The alum data presented in Figures 1 through 3 agree with similar data reported by Murray and Larson (6). However, the analysis has been extended to smaller sized crystals which are significant in the determination of the kinetic order for the nucleation rate. It appears that the kinetic order of nucleation is somewhat less than that determined by them.

NUMERICAL SOLUTION OF SIZE DISTRIBUTION EQUATION

The transient size distribution equation, Equation (1), was solved by a numerical analysis on a digital computer. Making the following dimensionless substitutions:

$$x = L/r_o T_o \tag{10}$$

$$y = n/n_o^o \tag{11}$$

$$\theta = t/T_o \tag{12}$$

$$\phi = r/r_o \tag{13}$$

Equation (1) simplifies to

$$\frac{\partial y}{\partial \theta} = -\phi \frac{\partial y}{\partial x} - y \frac{T_o}{T} \tag{14}$$

and the steady state equation, Equation (3), reduces to

$$y_o = \exp(-x) \tag{15}$$

Equation (15) is equivalent to an initial steady state crystal size distribution at a reference production rate before a disturbance in the distribution is caused by a step change in production rate.

Dimensionless nucleation and growth rate functions were obtained by performing the corresponding dimensionless substitutions on Equations (11) and (13). Thus, at constant suspension density we obtain

$$y^o = n^o/n_o^o = (r/r_o)^{i-1} = \phi^{i-1} \tag{16}$$

and

$$\phi = \frac{T_o \int_0^\infty x^2 e^{-x} dx}{T \int_0^\infty x^2 y dx} = \frac{2 T_o/T}{\int_0^\infty x^2 y dx} \tag{17}$$

Equation (14), solved with the initial and boundary conditions, Equations (15) and (16), predicted the transient response of the population density as the population adjusted from one steady state production rate to another. Only first order finite difference approximations were used in this analysis.

UNSTEADY STATE RESULTS

Data were collected for unsteady state operating conditions for the three crystal systems. A transient response was forced by a step decrease in residence time (a step increase in production rate). The crystallizer was first operated at 45 min. residence time for 20 drawdown times, then a step change to 15 min. residence time was made. Data were then collected for an additional twenty residence times.

Figures 7, 8, and 9 show the resulting transients as functions of dimensionless population density and dimensionless time with parameters of dimensionless size. Experimental operating conditions are tabulated in Table 1.

The figures show that the step change introduced a definite disturbance in the size distribution. This disturbance first occurred as a shower of nuclei and then grew through the larger size fractions. Steady state was again approached in an additional 20 residence times, correspondng to a total dimensionless time of 26 2/3. The respective locations of the various size fractions were also displaced. The larger sized crystals were degraded; the smaller crystals were enhanced. Thus, the net effect was an overall degradation of the crystal size distribution. The degree of degradation was a function of the crystal system with alum only slightly affected, ammonium sulfate moderately affected, and sodium chloride greatly affected. The total time required to approach steady state was also a function of the systems, sodium chloride had the slowest approach, alum the fastest.

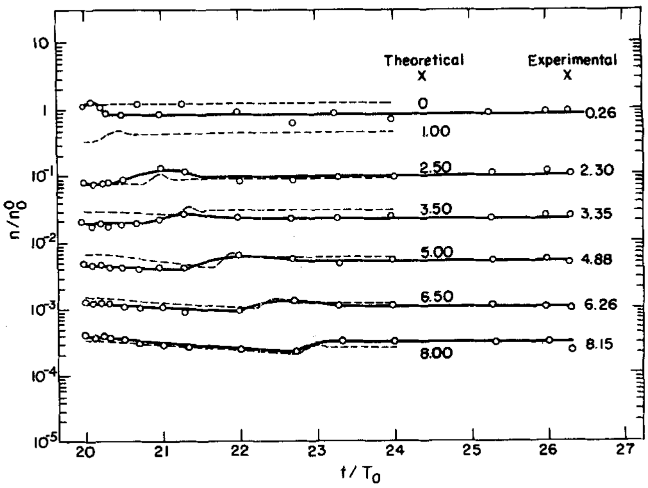

Fig. 7. Experimental and theoretical transient response of crystal population density for a step change in production rate, $T_o/T = 3.0$, alum-ethanol-water, $i = 1.25$, $T_o = 45$ min.

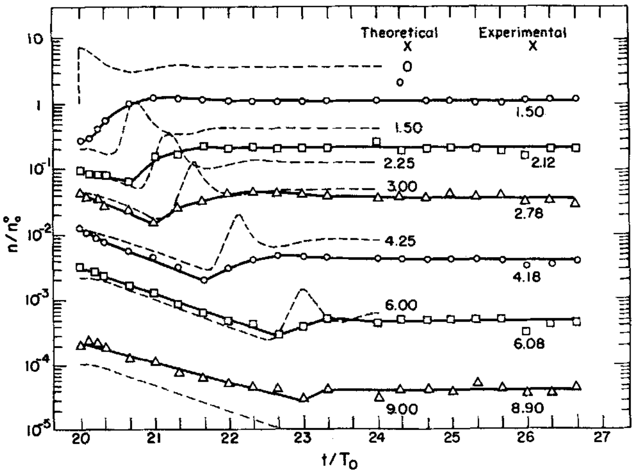

Fig. 8. Experimental and theoretical transient response of crystal population density for a step change in production rate, $T_O/T = 3.0$, ammonium sulfate-methanol-water, $i = 3.0$, $T_O = 45$ min.

Equation (14) was solved for various numerical values of the kinetic order of the nucleation rate. The curve was fitted to the experimental data by varying the kinetic order of nucleation only. The results of this analysis are also shown by Figures 7 and 8. A kinetic order for the nucleation rate of 1.25 for the alum system and 3.0 for the ammonium sulfate system is seen to correlate with the experimental transient data. The initial values and the final values of the population densities for the various crystal size fractions are seen to agree with that predicted theoretically. In addition, the model predicts the degradation of crystal size before a size fraction passes through its minimum value. However, the degree of overshoot predicted by the model, and experienced experimentally, are significantly different; but the time at which this maximum occurs is closely predicted. Refinements in the empirical power models used for crystal growth and nucleation rates may result in a reduction of the degree of overshoot.

The numerical solution's stability was found to be a function of the kinetic order of the nucleation rate. The higher kinetic order required to analyze the sodium chloride system was such that an unstable numerical solution resulted. However, the similarity of experimental data strongly suggests that these data are of the form predicted by the theoretical model of Randolph and Larson (7). Consequently, a stable numerical solution would be expected to approximate the experimental observations.

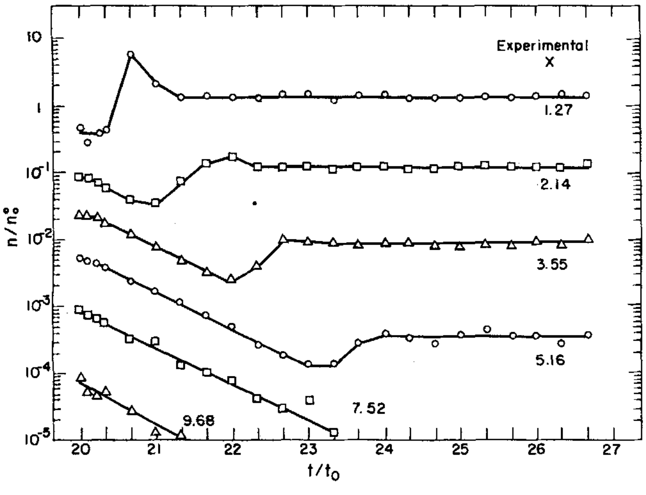

Fig. 9. Experimental transient response of crystal population density for a step change in production rate, $T_O/T = 3.0$, sodium chloride-ethanol-water, $T_O = 45$ min.

The observed degree of size degradation of the larger sized crystals is more pronounced than that observed for the other two systems. Thus, the data strongly indicate a higher kinetic order for the nucleation rate.

Murray and Larson (6) analyzed similar transient data for the alum system, in terms of moment equations, which are defined by the following relationships:

$$N_T = \int_0^\infty n dL \tag{18}$$

$$L_T = \int_0^\infty nL dL \tag{19}$$

$$A_T = K_a \int_0^\infty nL^2 dL \tag{20}$$

$$M_T = K_v \int_0^\infty nL^3 dL \tag{21}$$

This type of analysis is readily performed by analog computation, but possesses a major disadvantage. Namely, the moments are total quantities, the total number of crystals and their total length, area, and mass, that are contained in a defined suspension volume. Experimentally, a significant percentage of the total number of crystals is contained in crystals that are too small to analyze with a high level of competence and, therefore, is experimentally undefined. The total mass of crystals, although accurately defined by laboratory analysis, remains constant for a step change in production rate. The length and area moments have a higher level of experimental competence than the numbers moment, but less than that of the mass moment. A numerical solution has the disadvantage of computational cost, but it has a major advantage in calculating theoretical data corresponding to crystal size fractions which may be analyzed by conventional methods.

DISCUSSION

The steady state and the transient evaluation methods for the kinetic order of the nucleation rate yield numerical results which are slightly different. In the steady state method, the magnitude of the kinetic order is due primarily to the apparent population densities of the nuclei, the intercepts of Figures 1 through 5. Experimental scattering of data makes the exact location of these intercepts difficult to determine. Furthermore, since the coordinate is logarithmic, relatively small variations in the construction of the straight lines have correspondingly large affects upon the numerical values of the nuclei population densities without appreciably affecting the value of the growth rates. The transient method does not directly require extrapolation of experimental data to zero size although the procedure inherently assumes that the nuclei and the larger sized crystals form a continuous distribution. But, the method is restricted by the value of the nuclei population density at steady state through the normalization of experimental data. The probable error thus introduced is less significant than that resulting from the steady state analysis. The error introduced by this variable would simply shift the family of curves to a higher or lower value, depending on the sign of the error. Thus, a significant error would be obvious after a comparison with the model.

The transient tests vividly indicate the dynamic response of crystal size distribution as it adjusts from one equilibrium distribution to another. The data required are more laborious to obtain than those required for steady state analysis, but such data contain a significant part of the data required for the steady state analysis. Furthermore, the transient data provide a means for checking basic assumptions incorporated in the theoretical model, for example, McCabe's ΔL Law.

Some recent work by Sherwin, et al. (*10*) suggests that the damped nature of the experimental results, as compared to the model prediction, is due to the fact that nuclei were not close to zero size as assumed by the model. In order to get such an effect as described by them, the alum nuclei would have to have been 1.4μ in diameter, clearly much larger than existing theories predict.

The theoretical model, as shown by Figures 9 and 10, shows that for a step increase in production rate, an instantaneous increase in the nuclei population density results. This transient then grows its way through the other size fractions. By recalling the definition of y^o, Equation (16), and the constraint that crystal growth rate is a function of supersaturation, one may observe that the transient corresponding to the nuclei, $x = 0$, is also indicative of the level of supersaturation. It is interesting to note that the level of supersaturation for these systems approached steady state conditions in less than three drawdown times, a dimensionless time of one.

The nuclei that were formed at the time of the maximum nucleation rate were the seeds for the crystals that formed the maximum of each transient. Due to the increased growth rate of the system and to the fact that a fraction of the seeds in the form of nuclei and small crystals were removed from the crystallizer in its effluent, the population density decreased as the seeds grew to larger sizes.

A method for determining the growth rates of individual size fractions follows: the growth rate r of a size fraction may be represented by

$$r = \Delta L/\Delta t \tag{22}$$

ΔL may be calculated from adjacent size fractions, utilizing the definition of x, Equation (10); Δt may be determined from the dimensionless time that was required for the crystal to grow from one size fraction to a larger one.

Such a calculation showed that all size fractions did have a constant growth rate that was independent of their respective sizes. However, if the crystal distributions were such that larger crystals were grown than those observed in this investigation, the validity of this assumption would have to be verified. The basic numbers balance equation is flexible, and, if necessary, it may be adapted to a model for crystal growth rate that is dependent on crystal size.

SUMMARY

For the three crystal systems, growth and nucleation kinetics were determined from steady state and from transient data. It was shown that the steady state crystal size distribution is a linear function of the log of population density vs. crystal size. Furthermore, a method was discussed from which nucleation kinetics may be defined.

Experimental transient data, that resulted from a step change in production rate from an initial steady state size distribution, were collected under closely controlled experimental conditions. The data vividly demonstrate that such a step disturbance initially creates a shower of nuclei which grow in a definable manner to form a new steady state size distribution. These dynamic responses clearly indicate the oscillatory nature of similar responses observed in commercial equipment. The degree of crystal size degradation was shown to be widely different for the three systems.

With the use of the dynamic equations developed by previous authors and an initial steady state size distribution, the transient behavior of crystal size distribution that resulted from a step disturbance in production, was calculated by a numerical analysis. The theoretical model was shown to predict the observed experimental transient responses, thus providing an additional method for defining the kinetic order of the nucleation rate.

Simple empirical power models for growth rate and nucleation rate as a function of supersaturation were assumed in the investigation. Until further investigations warrant the use of more complex, fundamental models, the basic approach presented here can be used to correlate experimental data from which information on the basic and as yet undefined, mechanism for crystal formation and growth may develop for a continuous, mixed crystal suspension.

ACKNOWLEDGMENT

The authors gratefully acknowledge the support of the National Science Foundation Research Grant G2156.

NOTATION

A_T = total crystal area, sq. mm.
C_i = input feed concentration
C_o = mother liquor solute concentration
i = kinetic order of nucleation rate
K = proportionality constant
K_a = area shape factor
K_v = volumetric shape factor
L = average crystal diameter, mm.
L_d = dominant particle size, mm.
L_T = total length of crystals, mm.
M = suspension density—mass of crystals suspended in a given volume of magma slurry, g./ml.
M_T = total mass of crystals, g.
N = number of crystals, No./ml.
N_T = total number of crystals, No.
N^o = number of nuclei, No./ml.
n = crystal population density, No./mm.
n^o = nuclei population density, No./mm.
n_o^o = nuclei population density at steady state, No./mm.
r = linear crystal growth rate, mm./hr.
r_o = linear crystal growth rate at steady state, mm./hr.
T = residence time, hr.
T_o = steady state reference residence time, hr.
t = time, hr.
V = volume of crystallizer, ml.
x = dimensionless crystal size
y = dimensionless population density
θ = dimensionless time
ρ = crystal density, g./ml.
ϕ = dimensionless growth rate

LITERATURE CITED

1. Bransom, S. H., W. J. Dunning, and B. Millard, *Discussions Faraday Soc.*, **5**, 83 (1949).
2. Larson, M. A., D. C. Timm, and P. R. Wolff, *AIChE J.*, **14**, 448 (1968).
3. McCabe, W. L., *Ind. Eng. Chem.*, **21**, 112 (1929).
4. ———, and R. P. Stevens, *Chem. Eng. Prog*, **47**, 168 (1951).
5. Murray, D. C., and M. A. Larson, *AIChE J.*, **11**, 728 (1965).
6. Randolph, A. D., *ibid.*, 424 (1965).
7. ———, and M. A. Larson, *ibid.*, **8**, 639 (1962).
8. Robinson, J. N., and J. E. Roberts, *Can. J. Chem. Eng.*, **35**, 105 (1957).
9. Saeman, W. C., *AIChE J.*, **2**, 107 (1956).
10. Sherwin, M., Katz, S. Shinnar, S., *ibid.*, **13**, 1141 (1967).

Manuscript received July 29, 1967; revision received October 6, 1967; paper accepted October 9, 1967.